Ecosphere. **Can we detect ecosystem critical transitions and signals of changing resilience from paleo-ecological records?** Taranu Z.E., S.R. Carpenter, V. Frossard, J.-P. Jenny, Z. Thomas, J.C. Vermaire, and M.-E. Perga

Appendix 1. Supplemental figures

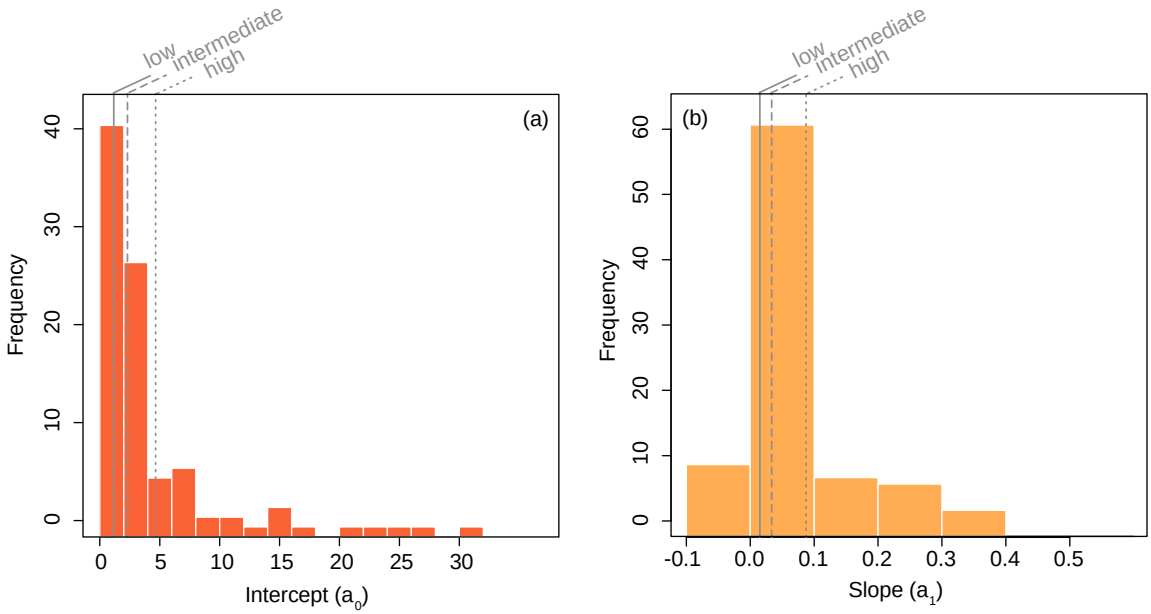

Figure S1. Histogram of (a) intercept, a_0, and (b) slope, a_1, of the sedimentation rate model from cores synthesized by Taranu et al. (2015). Sedimentation rate coefficients of example cores with relatively low (1st quartile: $a_0 = 1.28$, $a_1 = 0.015$), intermediate (median: $a_0 = 2.24$, $a_1 = 0.034$), and high (3rd quartile: $a_0 = 4.35$, $a_1 = 0.088$) compression are shown by grey solid, dashed, and dotted lines, respectively.

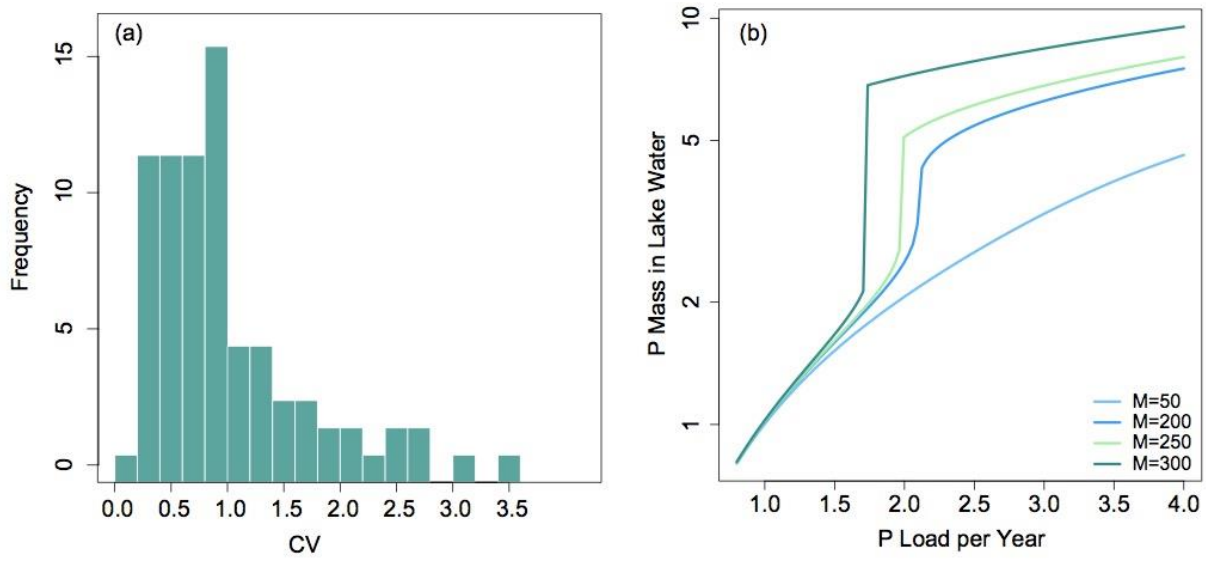

Figure S2. (a) Histogram of the coefficient of variation, CV, of cyanobacterial pigment concentrations from cores synthesized by Taranu et al. (2015). (b) Examples of deterministic eutrophication models with incremental sediment phosphorus mass (i.e. from non-critical to critical transitions).

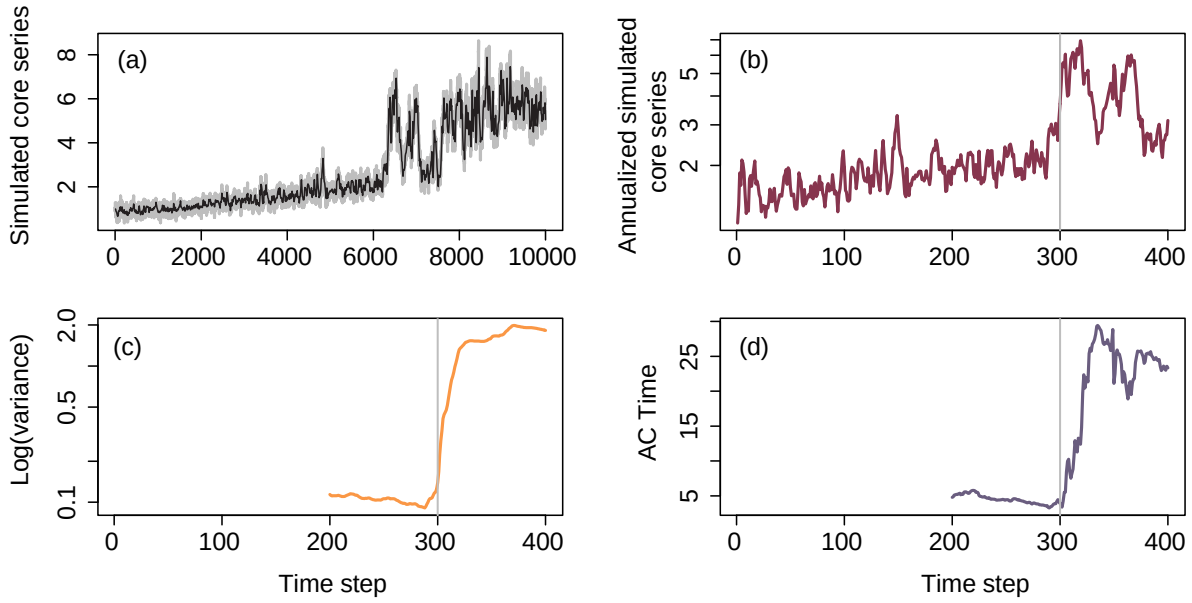

Figure S3. Simulated time series of critical slowing down (scenario 3: M = 225, σ = 0.15, v = 0.15) from the P load and lake eutrophication model. (a) Annualized time series (black) plotted over the 0.1-year series (grey). (b) Annualized time series truncated to 300 years prior and 100 post the SETAR threshold (re-scaled axis is shown). (c) Rolling window (*n*/2 time steps) variance and (d) lag-1 autocorrelation, presented as [1/ log(lag-1 autocorrelation coefficient)], of the truncated 400 year series. The SETAR switchpoint is shown by the grey line in panels (b-d).

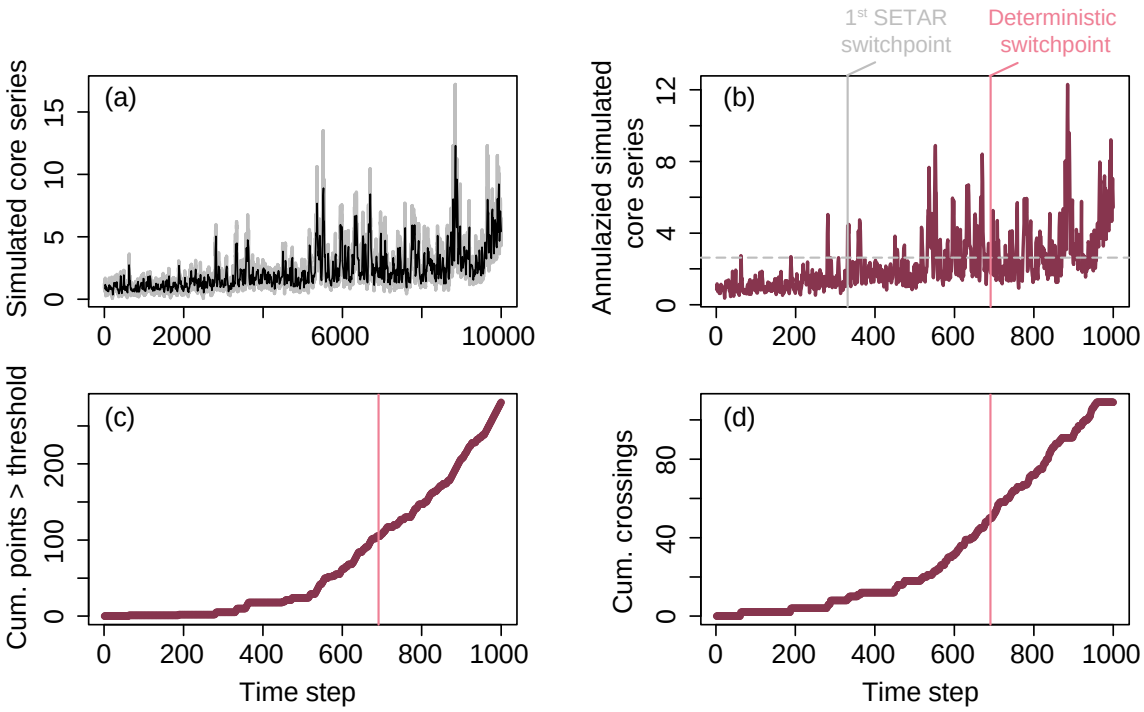

Figure S4. Simulated time series of flickering with high ecosystem noise (M = 225, σ = 0.45, v = 0.15). (a) Annualized time series (black) plotted over the 0.1-year series (grey). (b) Comparison of the true deterministic switchpoint (light red line) and the first SETAR crossing (grey line) for the annualized time series. (c) Cumulative sum of simulated values above SETAR threshold, where values above the threshold were assigned a value of 1, and those below were assigned a value of 0. (d) Cumulative number of times a state change occurs, where a 0 was assigned if the value either remained in an oligotrophic or eutrophic state from one time step to the next, otherwise a 1 was assigned.

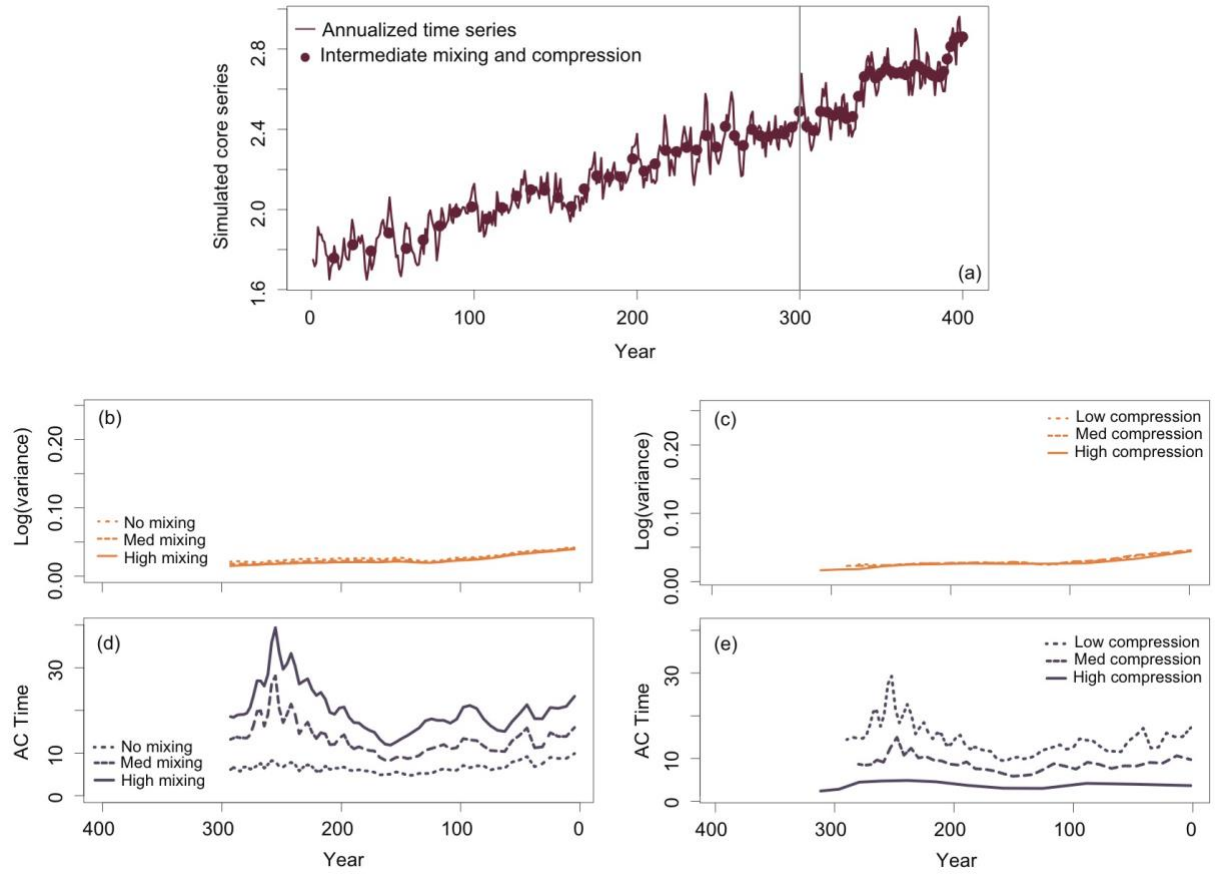

Figure S5. Effect of mixing and compression on the annualized control time series (scenario 1). See Fig. 2 for details.

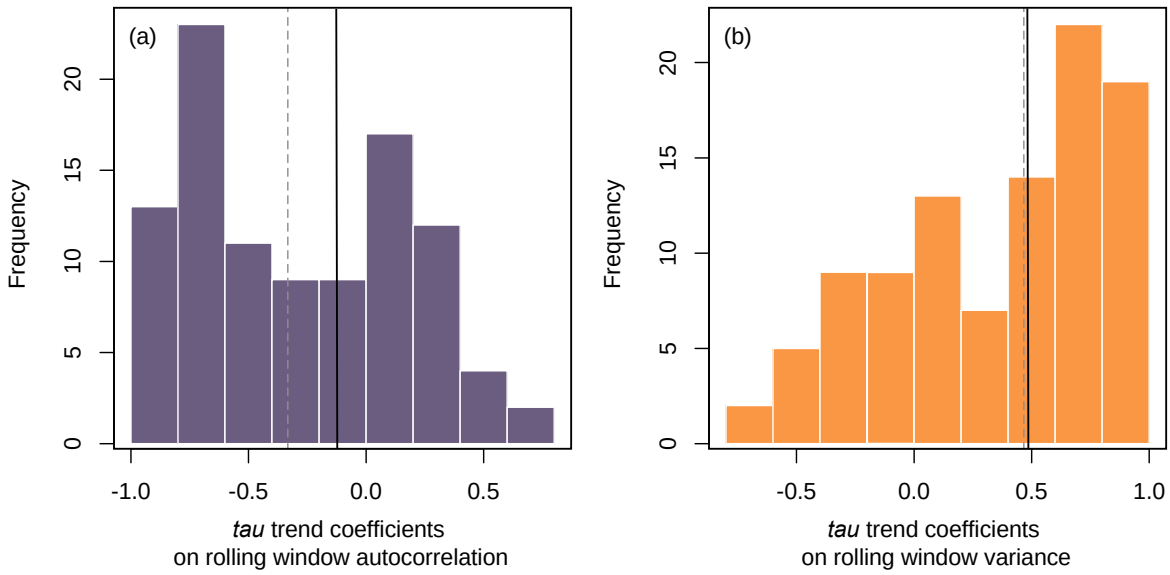

Figure S6. Summary histograms of the Kendall *tau* statistics on the rolling window (a) autocorrelation and (b) variance for 100 runs of the critical slowing down scenario (M = 225, σ = 0.15, v = 0.15) with intermediate mixing and intermediate compression. The rolling window length was decreased from 28.5 (*n*/2 time steps) to 21 to provide at least 10 data points for the Kendall *tau* statistic, which was calculated from the start of the rolling window series (time step 240) to the SETAR switchpoint (time step 300). Results from the selected example (Fig. 2) are shown by the black solid lines and the median of the 100 runs are shown by the grey dashed lines.

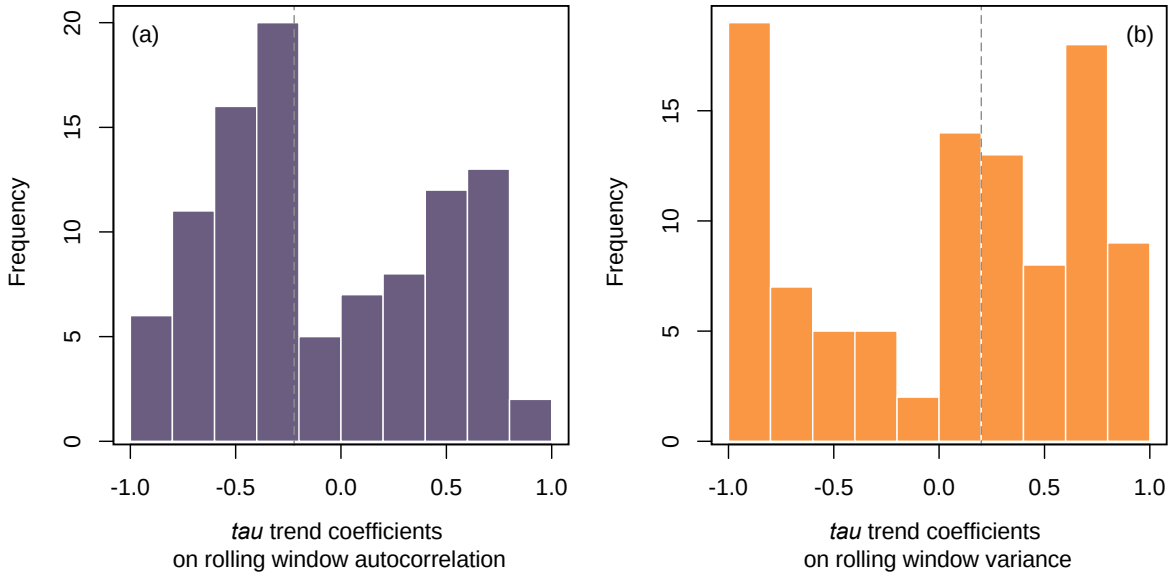

Figure S7. Summary histograms of the Kendall *tau* statistics on the rolling window (a) autocorrelation and (b) variance for 100 runs of the critical slowing down scenario with intermediate mixing and low compression. The rolling window length was decreased from 57.5 (n/2) to 45 to provide a series that covered the same time frame as in Fig. S6 (i.e. from time step 240 to 300). The median of the 100 runs are shown by the grey dashed lines.

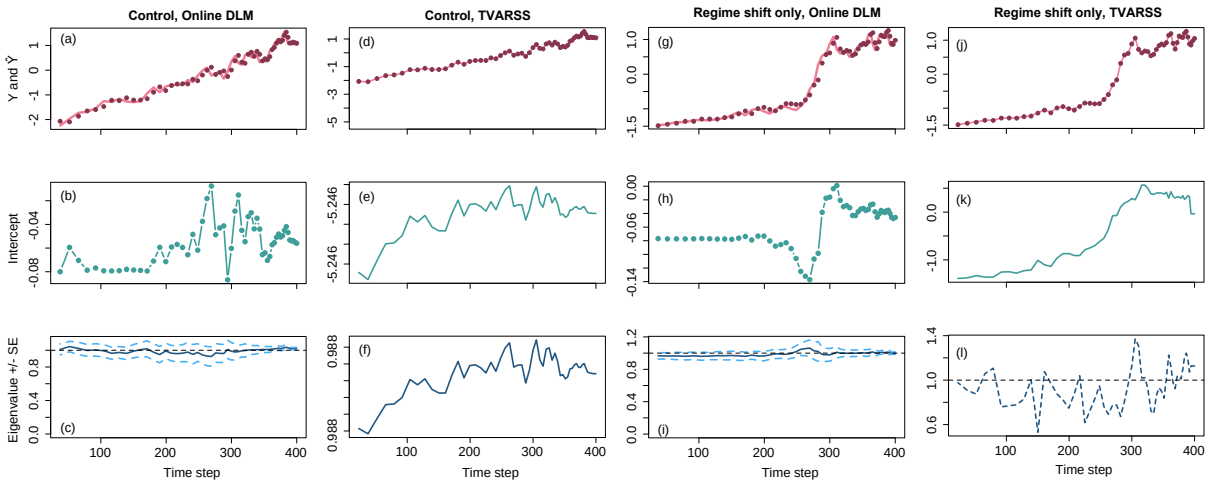

Figure S8. Online DLM and TVARSS results for the (a-f) control (scenario 1: M = 125, σ = 0.05, v = 0; optimal online DLM: AR(1); optimal TVARSS: AR(2)), and (d-f) regime shift only (scenario 2: M = 200, σ = 0.05, v = 0; optimal online DLM: AR(1); optimal TVARSS: AR(3)) sediment core simulations with intermediate core mixing and compaction (*n* = 57). The 400-year time series (dark red points), goodness of fit (light red line), intercept (green line), and eigenvalue (blue line) are shown for each scenario and modeling approach.

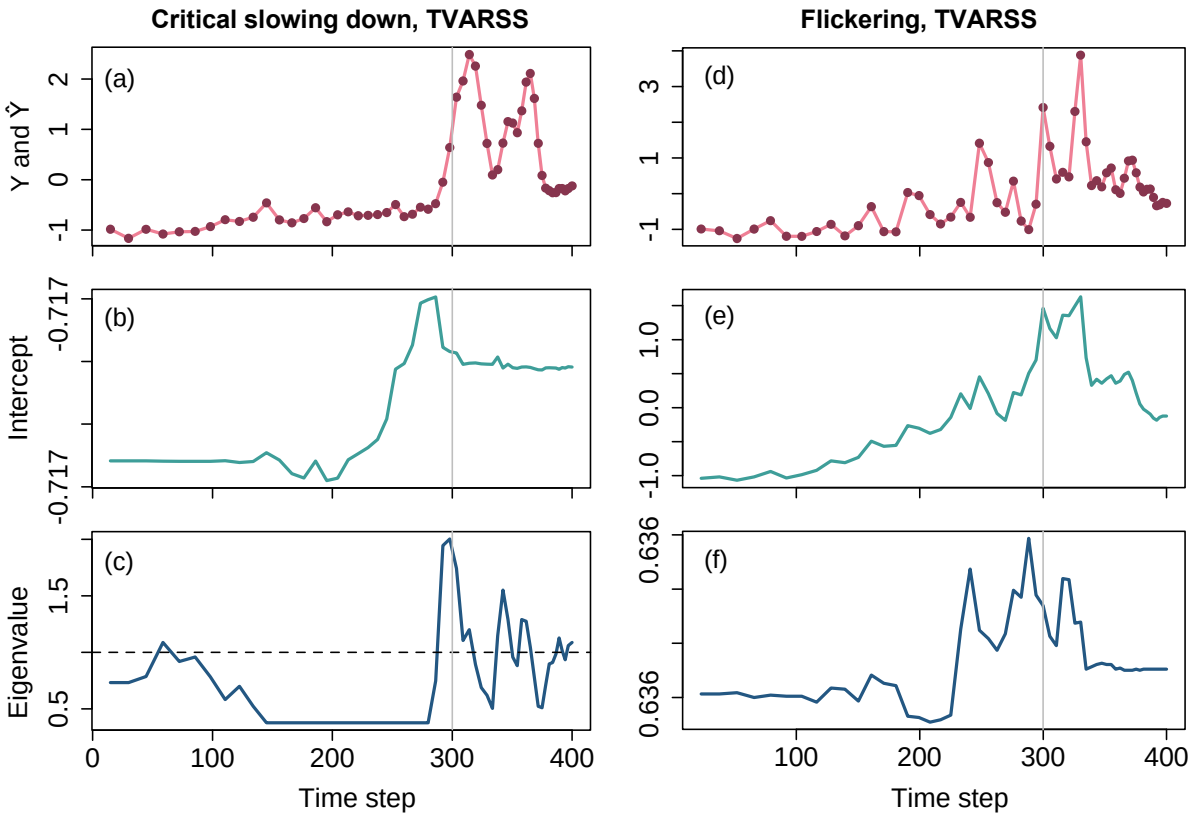

Figure S9. Summary of TVARSS for the (a-c) critical slowing down (scenario 3: M = 225, σ = 0.15, v = 0.15) and (d-f) flickering (scenario 4: M = 225, σ = 0.45, v = 0.15) sediment core simulations with intermediate mixing and compression. The time series (dark red points), goodness of fit (light red line), intercept (green line), and eigenvalues (blue line) are shown for each scenario.

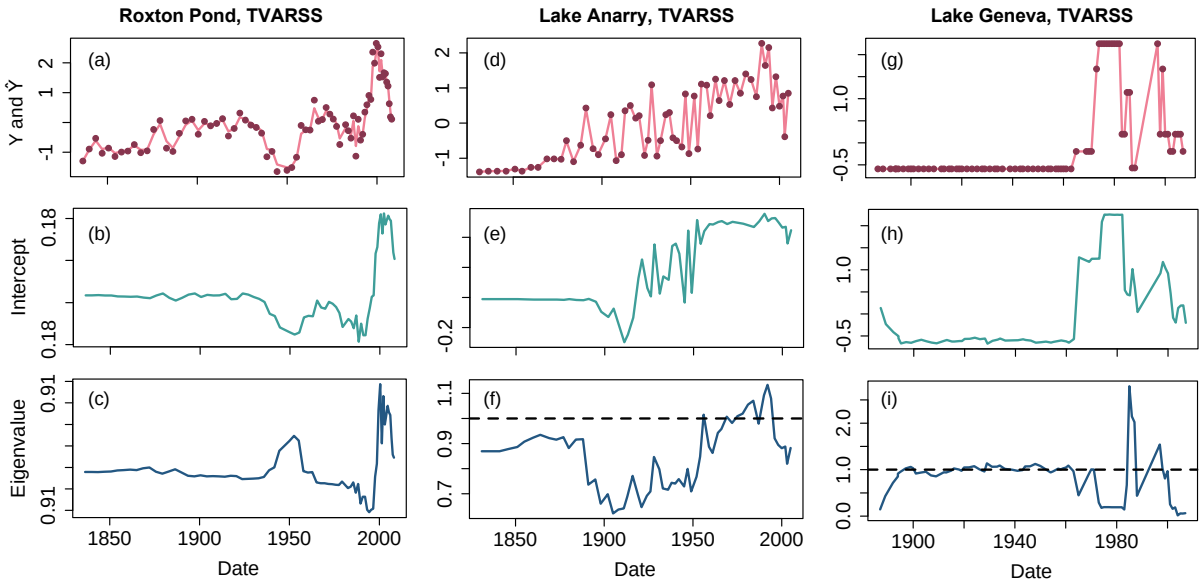

Figure S10. Summary of TVARSS for (a-c) Roxton Pond (optimal model: AR(1)), (d-f) Lake Anarry (optimal model: AR(3)) and (g-i) Lake Geneva (optimal model: AR(1)). The time series (dark red points), goodness of fit (light red line), intercept (green line), and eigenvalue (blue line) are shown for each lake. Note that for Lake Geneva, we included winter temperature as a covariate to control for the sharp increase in the response; that is, the increase in 1970 followed by 10 years of no change caused a challenge for TVARSS as the AR parameters follow a random walk and are limited in their rates of change. The covariate was thus used to capture the big jump.